metals

Article

Melting and Flowing Behavior of Mold Flux in a Continuous Casting Billet Mold for Ultra-High Speed

Jie Yang [1,*], Dengfu Chen [1,*], Fengting Qin [2], Mujun Long [1] and Huamei Duan [1]

1 Laboratory of Metallurgy and Materials, College of Materials Science and Engineering, Chongqing University, Chongqing 400044, China; longmujun@cqu.edu.cn (M.L.); duanhuamei@cqu.edu.cn (H.D.)

2 Department of Metallurgical and Chemical Engineering, Jiyuan Vocational and Technical College, Jiyuan 459000, China; qinfengting@163.com

* Correspondence: yangjie2018@cqu.edu.cn.com (J.Y.); chendfu@cqu.edu.cn (D.C.); Tel.: +86-133-2246-6016 (J.Y.); +86-023-6510-2467 (D.C.)

Received: 8 July 2020; Accepted: 17 August 2020; Published: 28 August 2020

Abstract: High casting speed coincides with the development trend of billet continuous casting, which significantly changes the casting characteristics. A mathematical model of the billet mold, which includes multiphase fluid flow, transient heat transfer, and solidification during ultra-high speed of the casting process was developed. The model is first applied to investigate the flow field of molten steel in the mold, studying the influence of steel flow upon the melting and flowing behavior of mold flux. The temperature and velocity distributions of the flux pool that formed above the molten steel surface are described. A parametric study on the melting temperature and viscosity of mold flux on liquid flux thickness and flow velocity is then carried out. Finally, the model is used to derive the relationship between interfacial tension and level fluctuations. The predictions provide an improved understanding of the melting and flowing behavior of mold flux in the billet mold and give the guidance for the design and optimization of mold flux for ultra-high speed of billet casting.

Keywords: ultra-high casting speed; billet mold; mold flux; heat transfer; fluid flow

1. Introduction

The increase of the casting speed has always been the goal of efficient continuous casting. Ultra-high speed has been one of the most distinguishing characteristics of billet continuous casting, which is also the basis and premise of billet endless rolling. For ultra-high speed of billet casting, the substantial increase in the flow rate of molten steel will significantly change the flow and heat transfer behaviors in the mold. Optimal performance of mold flux is critically important to match the heat transfer and lubrication conditions required in the mold for ultra-high casting speed.

The powder slag spread on the molten steel surface melts into a liquid layer or a flux pool. The liquid flux infiltrates into the channel between the mold and the shell, which rapidly freezes against the cooling mold wall and reduces the heat flux across the gap, while those close to the shell remain liquid to be consumed. The molten steel initially solidifies at the meniscus, where the heat flux and fluid flow behaviors determine the ultimate quality of the steel [1,2]. Some numerical models focusing on the phenomenon in the meniscus region assumed the constant meniscus profile based on the classic Bikerman equation [3–6]. Okazawa and Kajitani [7,8] simplified the flux channel between the mold wall and the solidified shell into a non-parallel channel to clarify the effect of mold oscillation on the slag infiltration. Since the consumption rate is an index to evaluate the shell lubrication, which depends on the layer thickness and viscosity gradients across the liquid layer, many researchers have measured slag consumption as related to casting parameters [9–11]. Shin et al. [12] proposed an empirical equation on the basis of extensive plant measurements, in which the total slag consumption was divided into two components—lubrication and oscillation mark consumption. The predictions from this model show a good consistency with the trends of casting parameter effects on flux consumption of plant measurements and other works.

The mold flux in the mold experiences the process of melting, resolidifying, and being consumed. Therefore, the melting and flowing behavior in the pool is an indispensable prerequisite for the lubrication and heat transfer of the thin gap between the mold and the steel. The study on slag melting as heat transfer in the slag layers above the molten steel has developed from one-dimension to three-dimensions [13,14]. The thermal properties used in computational models were varied with composition and temperature according to empirical equations or measurements. Jonayat and Thomas [15] presented a transient model of flux flow at the meniscus, which is used to study the casting condition effects on slag infiltration. Lopez et al. [16,17] developed a mathematical model of multiphase flow and heat flux in the continuous casting mold, which is applied to predict the complex phenomena taking place in the meniscus region including the formation of slag layers, slag infiltration, and initial solidification. However, previous researches on heat transfer and flow of mold flux in the mold mainly fixed the shape of slag bed or flux channel, and the casting speed in the model calculation was low. The evolution behavior of mold flux in a billet mold at ultra-high casting speed has not yet been involved.

The rapid melting and uniform distribution of mold flux in the billet mold is essential for ultra-high speed continuous casting. The current work presents a computational model of the billet mold, which couples mold flux and steel flow with heat transfer and solidification. This transient model is used to describe the melting and flowing behavior of mold flux in a billet mold for ultra-high casting speed. A parametric study is then carried out to elucidate the influences of a variety of flux properties on liquid flux thickness, flow velocity and level fluctuations. The model predictions in this study allow guidance for the evaluation and design of mold flux for ultra-high speed continuous casting.

2. Model Development

2.1. Model Description

In order to investigate the melting and flowing behavior of mold flux in a billet mold for ultra-high speed, a transient model that consists of multiphase flow and heat transfer models was developed in this work. The Navier–Stokes equations are solved for the multiphase flow, where the Volume of Fluid (VOF) model is coupled to determine the volume fractions of steel and mold flux. The Continuum Surface Force (CSF) method is applied to track the steel/slag interface. The realizable k-ε model is used to calculate the turbulent flow in the fluid region. The heat transfer model solves the Fourier equation, while the heat extracted from the copper wall is calculated by the water-cooled convection boundary.

$$\frac{\partial}{\partial t}(\alpha_{\mathrm{s}}\rho_{\mathrm{s}}) + \nabla\cdot\left(\alpha_{\mathrm{s}}\rho_{\mathrm{s}}\vec{v}\right) = \sum\left(\dot{m}_{\text{f-s}} - \dot{m}_{\text{s-f}}\right) \tag{1}$$

$$\frac{\partial}{\partial t}\left(\rho_{\mathrm{mix}}\vec{v}\right) + \nabla\cdot\left(\rho_{\mathrm{mix}}\vec{v}\vec{v}\right) = -\nabla p + \nabla\cdot\left[\mu_{\mathrm{mix}}\left(\nabla\vec{v} + \nabla\vec{v}^{T}\right)\right] + \rho_{\mathrm{mix}}g + \vec{S}_{\sigma} \tag{2}$$

$$\vec{S}_{\sigma} = \sigma_{\text{f-s}}\frac{\rho_{\mathrm{mix}}\kappa\nabla\alpha_{\mathrm{f}}}{\frac{1}{2}(\rho_{\mathrm{f}} + \rho_{\mathrm{s}})} \tag{3}$$

$$\frac{\partial}{\partial t}(\rho_{\mathrm{mix}}E_{\mathrm{mix}}) + \nabla\cdot\left(\vec{v}\left(\rho_{\mathrm{mix}}E_{\mathrm{mix}} + p\right)\right) = \nabla\cdot(K_{\mathrm{eff}}\nabla T) \tag{4}$$

The variables are explained in the list of nomenclature at the end of the paper. Full details of the mathematical model have been published in our previous works [18,19].

The schematic diagram of the three-dimension model with boundary conditions is given in Figure 1. The model domain is composed of a quarter of the Submerged Entry Nozzle (SEN) and a billet mold. The SEN is immersed 120 mm below the initial steel level that is set to 100 mm below the upper edge of mold wall. The initial layer of slag powder is spread on the liquid steel surface to calculate the slag bed and liquid flux pool. An air zone is placed on the slag powder top to model the effects of atmosphere pressure. A pressure boundary is applied at the mold outlet based on atmospheric pressure and hydrostatic pressure of steel. The molten steel with superheat of 20 K is poured into the mold through the SEN, and its flow rate is calculated according to the mass balance when the casting speed is 6 m/min. A convective condition on the outside of mold wall is used to take into account the heat removal by the cooling water. Heat flux through the SEN walls and symmetry planes are assumed to be zero. The model mesh size ranges from 50 μm to 2 mm. High degree of mesh refinement was applied at the slag area, include the interface between mold flux and molten steel.

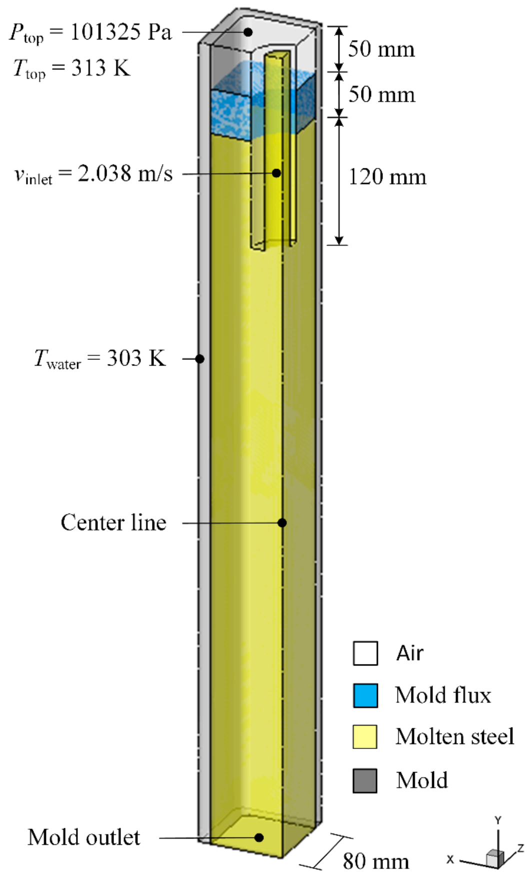

Figure 1. Schematic of model domain and boundary conditions.

The transient thermal flow model is solved in three steps. First, the isothermal flow model is run to develop the full flow pattern of molten steel and steel/flux interface. Next, the energy equations are activated to calculate the shell growth and slag melting. Finally, the complete system coupling casting speed and oscillation equation is solved, so the mold flux is allowed to infiltrate into the gap between the mold and the shell. The melting and flow behavior of mold flux in a billet mold for ultra-high casting speed is predicted based on the time-averaged results from this model. The solution procedure is the same when the flux property is varied in different runs.

The numerical approach used in this paper has been successfully applied to characterize the meniscus formation and slag infiltration phenomena in the slab casting mold and the conventional billet mold. Predicted slag film thicknesses, slag consumption, and heat fluxes show a good agreement with plant measurements and other models [20,21]. Previous work and other mathematical models validate the modelling method, which provides a basis for this study to accurately predict the mold flux behavior in the billet mold during ultra-high casting speed.

2.2. Material Properties

The materials properties in model calculation are listed in Table 1. In this study, the steel thermal conductivity is simulated using a linear function of temperature, while other properties of the steel are defined as constants. The constant composition is used to model the temperature-dependent properties of the mold flux, since the change in slag composition during the casting process is negligible. Figure 2 shows the temperature-dependent viscosity and thermal conductivity of the mold flux. The viscosity of the mold flux is greatly affected by temperature, and its characteristics during the melting and solidification processes are different. The slag powder on the steel top is modeled as it sinters and melts to the liquid, where the viscosity goes through a process of increasing first and then decreasing. The effective thermal conductivity of mold flux that comprises of conduction and radiation is used in the simulation. The thermal conductivity of slag powder is fixed at 0.3 W/m K below its sintering temperature [22]. Then, the conductivity gradually increases as air spaces disappear in the sintered layer when the temperature keeps going up. For the liquid flux, a constant effective thermal conductivity of 2 W/m K above the melting temperature is adopted [15,23]. To examine the effect of flux properties on melting and flowing behaviors, different melting temperatures and viscosities at 1573 K of mold flux are used in the model calculation whilst the other parameters are held constant. In addition to the standard interfacial tension between molten steel and mold flux of 1.35 N/m, the model is applied to determine the effect of varying interfacial tension from 1.10 to 1.60 N/m. The ranges are also given in the table.

Table 1. Materials properties.

Property	Value	Unit
Steel liquidus temperature	1790	K
Steel solidus temperature	1761	K
Steel latent heat	264	kJ/kg
Steel heat capacity	720	J/kg·K
Steel thermal conductivity	$19.32 + 8.35 \times 10^{-3} \times (T\text{-}273)$	W/(m·K)
Steel viscosity	0.0065	Pa·s
Steel density	7400	kg/m^3
Flux melting temperature	1413, 1363, 1313	K
Flux density	2600	kg/m^3
Flux viscosity at 1573 K	0.5, 0.3, 0.1	Pa·s
Interfacial tension between molten steel and mold flux	1.60, 1.35, 1.10	N/m
Mold thermal conductivity	387	W/(m·K)
Mold density	8900	kg/m^3
Mold heat capacity	390	J/kg·K

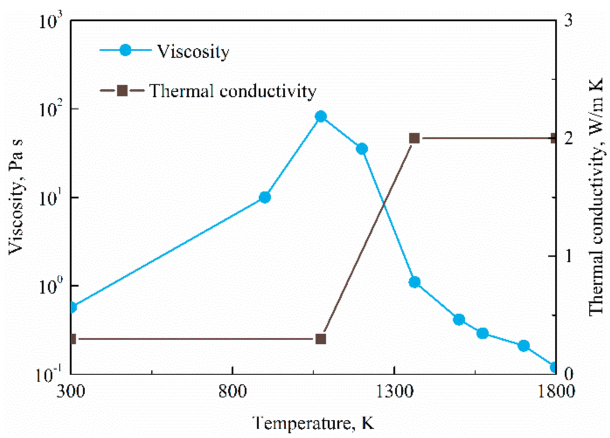

Figure 2. Temperature-dependent viscosity and thermal conductivity of mold flux.

3. Results and Discussion

3.1. Flow Field of Molten Steel

The increase in the flow rate of molten steel during high casting speed will enhance the interfacial disturbance as well as the convective heat transfer of mold flux. The steel flow field in the billet mold during the casting speed of 6 m/min is first investigated, as shown in Figure 3. The molten steel flows from the nozzle to the bottom of the mold with the thickening stream, which impacts on the inner surface of billet shell to split either upward or downward. The steel reaching the top flows to the mold center, generating a recirculation zone with the new steel stream from the SEN port. Therefore, the metal surface in the mold is high on the edge and low in the middle, of which the impact strength at the mold corner is the largest. Compared with the conventional casting speed, ultra-high casting speed results in a deeper impact depth of the steel flow as well as a higher level rise. The flow field of molten steel in the upper part of the mold has an important influence on the melting and flowing behavior of mold flux as discussed in more detail in the next section.

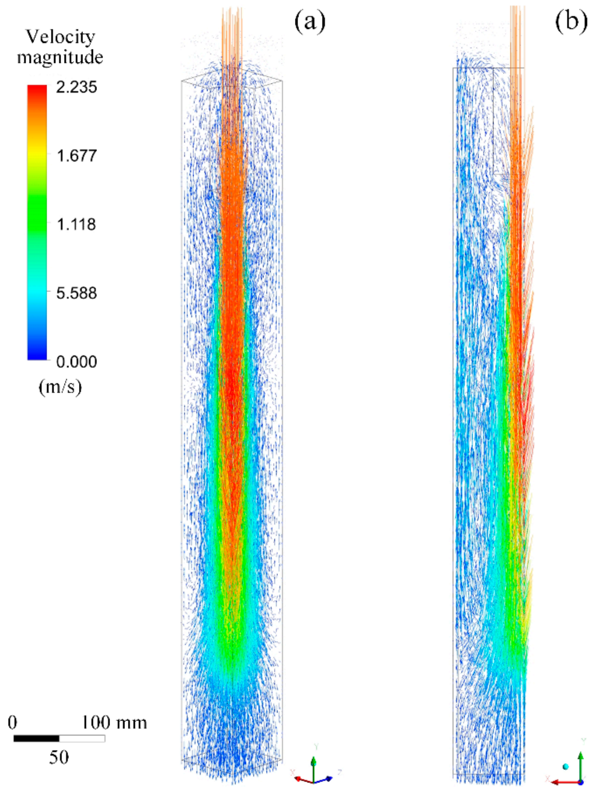

Figure 3. (**a**) 3D and (**b**) 2D flow field of molten steel in billet mold.

3.2. Temperature Distribution of Mold Flux

Figure 4 shows the temperature distribution at a plane located 5 mm above the steel surface. Naturally, low temperature is located around the mold under the forced cooling of the mold wall. There is a high temperature area between the nozzle and the mold corner in the liquid flux pool, corresponding to the impact position of the steel flow on the surface. Higher temperature promotes melting of mold flux, to produce an active region in the liquid flux pool, as marked A in the figure. Besides, the temperature of mold flux between the middle of the mold wall and the nozzle is lower due to the reduced convective heat transfer of molten steel and closer cooling distance from both sides, as marked I in the figure. This temperature difference in the liquid flux pool suggests that the slag powder should be added more often near the mold corner (region A) than in the middle of the mold (region I) during the billet continuous casting.

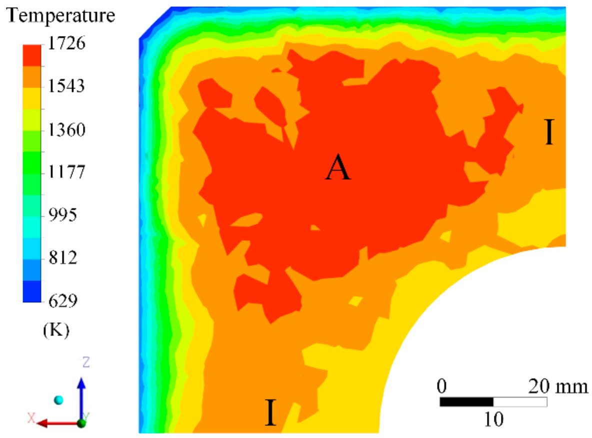

Figure 4. Temperature distribution at a plane located 5 mm above the steel surface.

Figure 5 presents the temperature distribution near the meniscus region at the symmetry plane. The steel stream provides heat to melt the slag powder on the molten steel surface, while the liquid flux close to the mold wall is cooled to form a solid phase that accumulates into a slag rim. The shape of slag rim matches the curvature of the meniscus and forms a flux channel with the meniscus profile as a result of the two-dimensional heat transfer. As the steel flow falls back, the vertical heat flux near the nozzle decreases, which leads to the isotherm of the mold flux to goes down with the declining metal level.

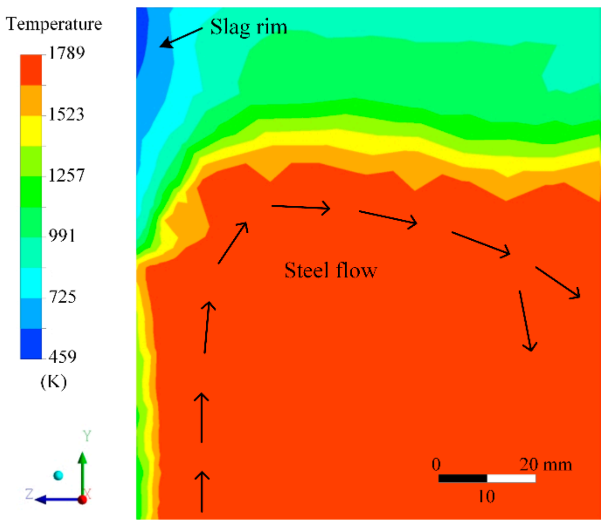

Figure 5. Temperature distribution near the meniscus region at the symmetry plane.

The typical profiles of molten steel and liquid flux in the billet mold are presented in Figure 6. A hump-shaped meniscus is created by the impact of the steel flow, then the steel/flux interface appears a valley near the SEN after a flat transition. This indicates that the areas around the mold and near the nozzle are greatly affected by the steel flow, thus it is more likely to cause surface defects related to severe interface fluctuations. For instance, the situation where the meniscus gets close to the slag rim will lead to abnormal cooling of the shell, increasing the possibility of deeper oscillation mark and hook formation [24]. In addition, a severe level drop near the nozzle may bring the liquid flux into the steel to result in slag entrapment in the solidified shell [25]. The slag rim corresponds to liquid flux that returns to solid state in colder area blow the solidification temperature, which is connected to the unmelted flux in the bed forming a sintered layer above the liquid pool. The depth of liquid pool determines the amount of liquid flux available to lubricate the shell. As described before, convection in the recirculating zone creates the thickest liquid flux layer in the middle of the nozzle and mold corner. The liquid layer between the middle of the mold wall and the nozzle is thinner, which is expected to be starved for flux infiltration. This thin position depends on the flow pattern developed in the upper mold and the fluidity of mold flux.

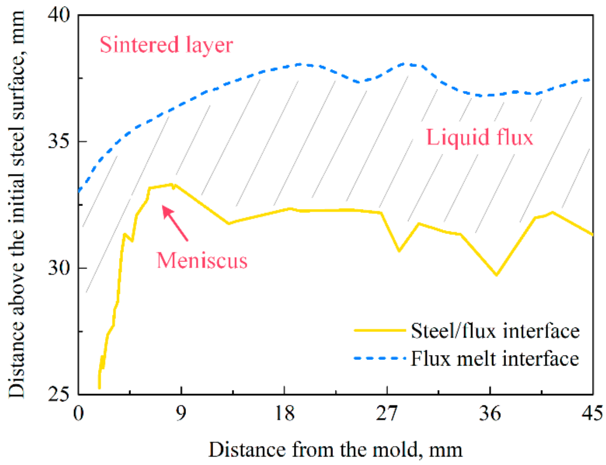

Figure 6. Profiles of molten steel and liquid flux.

3.3. *Velocity of Mold Flux in the Pool*

In order to clarify the flow phenomenon of mold flux in the liquid pool, the velocity distribution of mold flux in two directions at the symmetry plane is investigated. Figure 7 compares the velocity of mold flux in casting direction at three positions in the liquid flux pool. The velocity distribution above the flux channel is an inverted parabolic shape, where the mold flux infiltrates into the channel to be consumed quickly. The vertical velocity of mold flux in the upper part of the liquid pool is close, which decreases with the distance away from the flux gap. The velocity at the steel/flux interface fluctuates violently due to the disturbance of steel flow, especially near the nozzle.

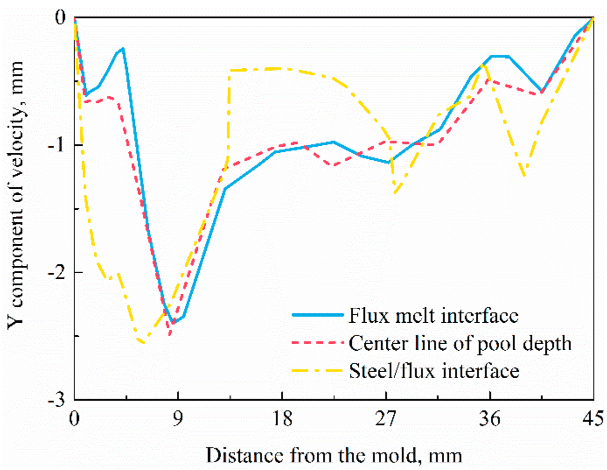

Figure 7. Velocity in casting direction of mold flux as a function of distance from the mold.

Figure 8 shows the velocity in the x direction of mold flux as a function of distance from the mold. The direction of the flux flow towards the mold wall is considered as positive. Apparently, the closer to the molten steel, the more active mold flux, so the faster flow rate. Since the mold flux near the mold wall mainly infiltrates into the flux channel, the velocity in the horizontal direction is small. The flow of mold flux away from the mold is variable. Some of the mold flux in the upper part of the liquid pool flows slowly to the mold, while others first flow down to the interface and then quickly move to the flux channel as a supplement. Therefore, the mold flux near the SEN has more residence time above the molten steel because of the slow melting and flowing process.

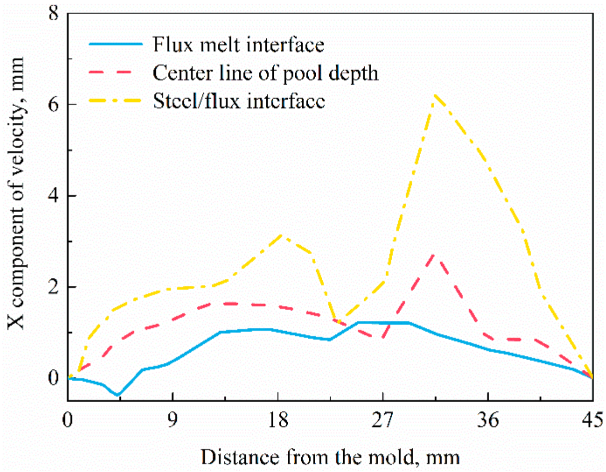

Figure 8. Velocity in x direction of mold flux as a function of distance from the mold.

It is found that the flow feature of mold flux in the billet mold is significantly different from that of the slab. There is a long channel toward the narrow face for the mold flux in slab mold, so the backflow of molten steel attempts to bring the flux toward the SEN to produce a separation in the flow field somewhere. This flow in the opposite direction drives the flux away from the mold wall to generate a recirculation zone in the flux pool [14]. However, the upward steel flow quickly falls after reaching the highest position, resulting in a low horizontal flow rate in the billet mold, which has little effect on the consumption flow to the flux channel. Therefore, the liquid flux flow in the billet mold is predominantly in the direction toward the mold wall. An opposing flow at the flux melt interface may appear at the edge of the slag rim due to the blocking of the slag rim. This phenomenon implies that if the slag rim grows overly, it will hinder the infiltration of mold flux to a greater extent.

3.4. Effect of Flux Properties

The effects of flux property on the liquid flux thickness and velocity are explored for better understanding the melting and flowing behavior of mold flux in the billet mold during the ultra-high casting speed. Figure 9 shows the effect of melting temperature on the liquid flux pool depth at the symmetry plane. In general, lower melting temperature of mold flux shifts the melt interface of the slag bed upward to form a deeper liquid pool. It should also be noted that further decreasing melting temperature will reduce the effect of increasing the thickness of the liquid flux layer. The general increase in liquid layer depths is expected to improve feeding to the middle of the mold wall.

For ultra-high speed continuous casting, sufficient pool depth is a guaranteed supply of liquid flux, and good fluidity is used to ensure the consumption flow into the flux channel. Figure 10 compares the velocities for mold flux with different melting temperatures. In order to diminish the influence of steel fluctuations and sintered layer melting, the velocity in the middle of the liquid flux pool is chosen to better reflect the effect of flux properties on the flux flow in the pool. It is found that lower melting temperature significantly increases the flow rate of the mold flux, especially near the meniscus, which will promote the consumption flow into the flux channel. This indicates that lower melting temperature permits larger velocity that generates more convective heat transfer from the steel/flux interface to the active region of the liquid flux pool.

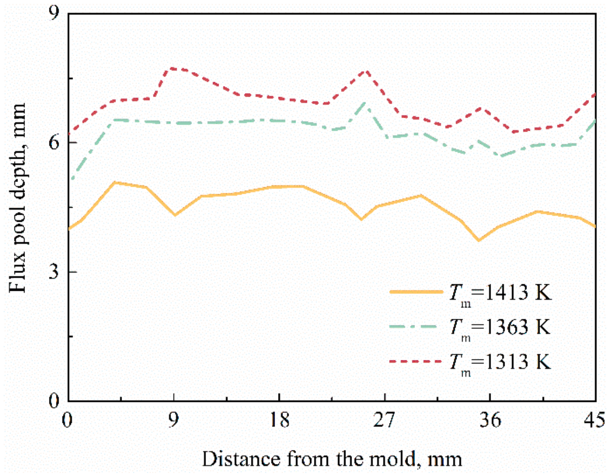

Figure 9. Effect of melting temperature on flux pool depth.

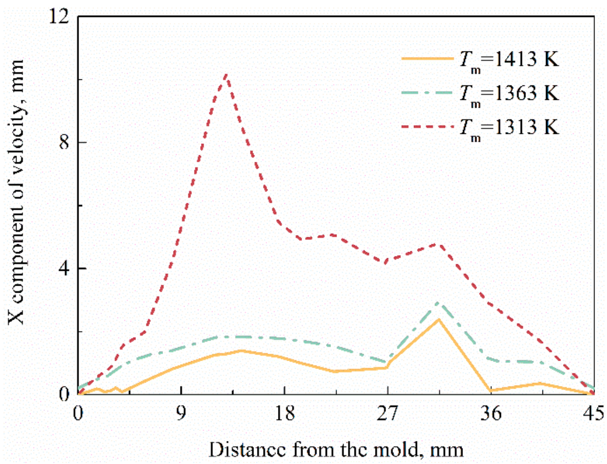

Figure 10. Effect of melting temperature on flow velocity of mold flux.

It is known that the flux consumption rate decreases with increasing casting speed, thus lower viscosity is usually used to obtain adequate flux consumption during high speed continuous casting. Figure 11 shows the effect of viscosity on the flow velocity of mold flux in the liquid pool. The lower viscosity increases the flow rate of the mold flux, contributing to the uniformity of heat transfer in the liquid pool. It is worth noting that since the liquid flux pool in the slab mold is more active, including a large recirculation zone, the lower flux viscosity will enhance the convective heat transfer in the flux pool, thereby deepening the local liquid flux layer. However, this change is not obvious in the flux pool of billet casting.

Although the interfacial tension between molten steel and mold flux depends more on the surface tension of molten steel, it has an important influence on the slag entrapment, meniscus depression, and flux infiltration [22,23]. Therefore, the effect of interfacial tension between molten steel and mold flux on the level fluctuations is examined, as presented in Figure 12. It should be pointed out that the predicted level fluctuations in this study are expected to be slightly lower than those from plant data, since the effect of mechanical vibration is not considered in the model calculation. However, the predictions are able to explain the relationship between the interfacial tension and level fluctuations. It can be seen from the decrease of the maximum fluctuations (Figure 12, right top), the higher interfacial tension is conducive to reduce the interface fluctuations. Moreover, the increase of the interfacial tension shows a good effect on stabilizing the liquid level near the nozzle, which decreases the incidence of severe level drop, minimizing the possibility of slag entrapment.

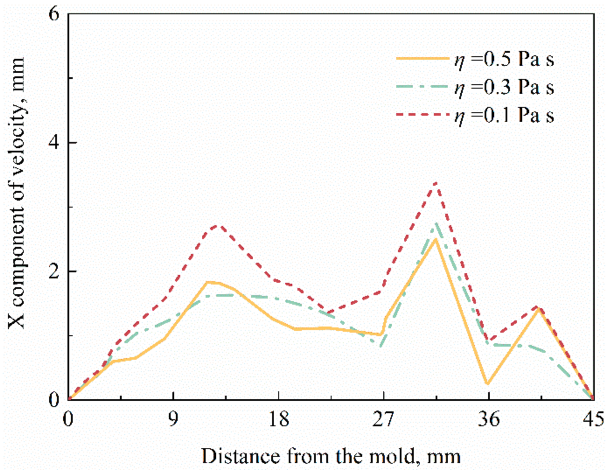

Figure 11. Effect of viscosity on flow velocity of mold flux.

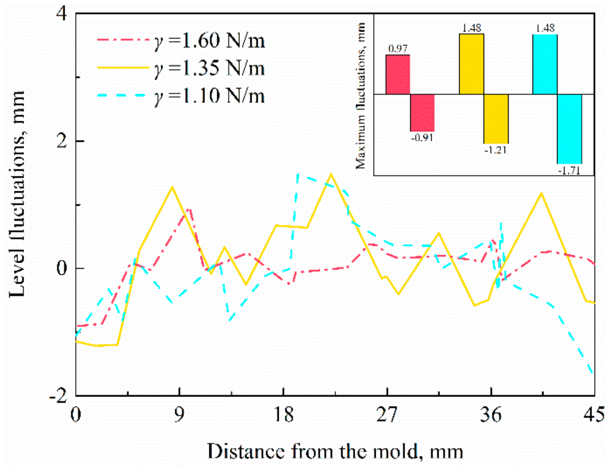

Figure 12. Effect of interfacial tension on level fluctuations.

4. Conclusions

The melting and flowing behavior of mold flux in a billet mold of continuous casting during ultra-high speed is characterized using a mathematical model that couples the fluid flow with heat transfer and solidification. The relationships between the mold flux properties and responses are investigated to provide insights into the evaluation of flux properties for ultra-high casting speed of billet mold. The main findings include the following.

1. The high speed steel flow produces a hump-shaped meniscus at the steel/flux interface and maximum in level fluctuations near the SEN.
2. An active region with higher temperature and thicker layer is generated near the mold corner in the liquid flux pool, corresponding to the impact position of the steel flow on the surface. In contrast, the flux temperature between the middle of the mold wall and the nozzle is lower due to the reduced convective heat transfer of molten steel and closer cooling distance from both sides.
3. Lower melting temperature of mold flux produces deeper liquid pool, which is expect to contribute to the consumption flow, especially the feeding to the middle of the mold wall. The decreases of melting temperature and viscosity permit larger velocity that generates more convective heat transfer from the steel/flux interface to the active region of the liquid pool.
4. Higher interfacial tension between molten steel and mold flux reduces the interface fluctuations, which is particularly conducive to decrease the incidence of severe level drop near the SEN, minimizing the possibility of slag entrapment.

Author Contributions: Conceptualization, J.Y. and D.C.; investigation, J.Y. and F.Q.; methodology, J.Y. and M.L.; data curation, J.Y. and H.D.; writing—original draft preparation, J.Y.; supervision, D.C. All authors have read and agreed to the published version of the manuscript.

Funding: This work was supported by the National Natural Science Foundation of China (grant numbers 51904046 and 51874060) and the Postdoctoral Science Foundation of Chongqing (grant number cstc2019jcyj-bshX0027).

Conflicts of Interest: The authors declare no conflict of interest.

Nomenclature

α	Phase fraction
ρ	Density
$\vec{v}$	Velocity vector
m	Mass transfer between the phases
p	Pressure
g	Gravitational force
μ	Viscosity
$\vec{S}_\sigma$	Momentum sink due to the interfacial tension
$\sigma_{\text{f-s}}$	Flux/steel interfacial tension
κ	Local surface curvature
E	Enthalpy
K	Thermal conductivity

References

1. Meng, Y.; Thomas, B.G. Heat transfer and solidification model of continuous slab casting: CON1D. *Metall. Mater. Trans. B* **2003**, *34*, 685–705. [CrossRef]
2. Lee, P.D.; Ramirez-Lopez, P.E.; Mills, K.C.; Santillana, B. Review: The "butterfly effect" in continuous casting. *Ironmak. Steelmak.* **2012**, *39*, 244–253. [CrossRef]
3. Takeuchi, E.; Brimacombe, J.K. The formation of oscillation marks in the continuous casting of steel slabs. *Metall. Mater. Trans. B* **1984**, *15*, 493–509. [CrossRef]
4. Schwerdtfeger, K.; Sha, H. Depth of oscillation marks forming in continuous casting of steel. *Metall. Mater. Trans. B* **2000**, *31*, 813–826. [CrossRef]
5. Yamauchi, A.; Emi, T.; Seetharaman, S. A mathematical model for prediction of thickness of mould flux. *ISIJ Int.* **2002**, *42*, 1084–1093. [CrossRef]
6. Yang, J.; Meng, X.; Wang, N.; Zhu, M. Oscillation-mark formation and liquid-Slag consumption in continuous casting mold. *Metall. Mater. Trans. B* **2017**, *48*, 1230–1247. [CrossRef]
7. Okazawa, K.; Kajitani, T.; Yamada, W.; Yamamura, H. Infiltration phenomena of molten powder in continuous casting derived from analysis using Reynolds equation part 2: Unsteady analysis. *ISIJ Int.* **2006**, *46*, 234–240. [CrossRef]
8. Kajitani, T.; Okazawa, K.; Yamada, W.; Yamamura, H. Cold model experiment on infiltration of mould flux in continuous casting of steel: Simulation of mould oscillation. *ISIJ Int.* **2006**, *46*, 1432–1441. [CrossRef]
9. Suzuki, M.; Suzuki, M.; Nakada, M. Perspectives of research on high-speed conventional slab continuous casting of carbon steels. *ISIJ Int.* **2001**, *41*, 670–682. [CrossRef]
10. Mills, K.C.; Fox, A.B.; Li, Z.; Thackray, R.P. Performance and properties of mould fluxes. *Ironmak. Steelmak.* **2005**, *32*, 26–34. [CrossRef]
11. Araki, T.; Ikeda, M. Optimization of mold oscillation for high speed casting—New criteria for mold oscillation. *Can. Metall. Q.* **1999**, *38*, 295–300.
12. Shin, H.; Kim, S.; Thomas, B.G.; Lee, G.; Park, J.; Sengupta, J. Measurement and prediction of lubrication, powder consumption, and oscillation mark profiles in ultra-low carbon steel slabs. *ISIJ Int.* **2006**, *46*, 1635–1644. [CrossRef]
13. Nakano, T.; Fuji, M.; Nagano, K.; Matsuyama, T.; Masuo, N. Model analysis of melting process of mold powder for continuous casting of steel. *Nippon Steel Tech. Rep.* **1987**, *34*, 21–30.
14. McDavid, R.M.; Thomas, B.G. Flow and thermal behavior of the top surface flux/powder layers in continuous casting molds. *Metall. Mater. Trans. B* **1996**, *27*, 672–685. [CrossRef]

15. Jonayat, A.S.M.; Thomas, B.G. Transient thermo-fluid model of meniscus behavior and slag consumption in steel continuous casting. *Metall. Mater. Trans. B* **2014**, *45*, 1842–1864. [CrossRef]
16. Ramirez-Lopez, P.; Lee, P.D.; Mills, K.C. Explicit modelling of slag infiltration and shell formation during mould oscillation in continuous casting. *ISIJ Int.* **2010**, *50*, 425–434. [CrossRef]
17. Ramirez-Lopez, P.; Lee, P.D.; Mills, K.C.; Santillana, B. A new approach for modelling slag infiltration and solidification in a continuous casting mould. *ISIJ Int.* **2010**, *50*, 1797–1804. [CrossRef]
18. Yang, J.; Cai, Z.; Zhu, M. Transient thermo-fluid and solidification behaviors in continuous casting mold: Evolution phenomena. *ISIJ Int.* **2018**, *58*, 299–308. [CrossRef]
19. Yang, J.; Chen, D.; Long, M.; Duan, H. An approach for modelling slag infiltration and heat transfer in continuous casting mold for high Mn–high Al steel. *Metals* **2020**, *10*, 51. [CrossRef]
20. Yang, J.; Cai, Z.; Chen, D.; Zhu, M. Characteristics of slag infiltration in high Mn steel castings. *Metall. Mater. Trans. B* **2019**, *50*, 1104–1113. [CrossRef]
21. Yang, J.; Chen, D.; Long, M.; Duan, H. Transient flow and mold flux behavior during ultra-high speed continuous casting of billet. *J. Mater. Res. Technol.* **2020**, *9*, 3984–3993. [CrossRef]
22. Meng, Y.; Thomas, B.G. Simulation of microstructure and behavior of interfacial mold slag layers in continuous casting of steel. *ISIJ Int.* **2006**, *46*, 660–669. [CrossRef]
23. Ozawa, S.; Susa, M.; Goto, T.; Endo, R.; Mills, K.C. Lattice and radiation conductivities for mould fluxes from the perspective of degree of crystallinity. *ISIJ Int.* **2006**, *46*, 413–419. [CrossRef]
24. Ramirez-Lopez, P.; Mills, K.C.; Lee, P.D.; Santillana, B. A unified mechanism for the formation of oscillation marks. *Metall. Mater. Trans. B* **2012**, *43*, 109–122. [CrossRef]
25. Cho, S.; Thomas, B.G.; Kim, S. Effect of nozzle port angle on transient flow and surface slag behavior during continuous steel slab casting. *Metall. Mater. Trans. B* **2019**, *50*, 52–76. [CrossRef]